UDK 669.245:669.15-194:621.793
Original scientific article/Izvirni znanstveni članek

ISSN 1580-2949
Mater. Tehnol.

INVESTIGATION ON MICROSTRUCTURAL AND GEOMETRICAL CHARACTERIZATION OF COLD METAL TRANSFER HARDFACED INCONEL 718 ON MEDIUM CARBON STEEL

MIKROSTRUKTURNE PREISKAVE IN GEOMETRIJSKA KARAKTERIZACIJA TRDE PREVLEKE IZ Ni ZLITINE INCONEL 718 NA POVRŠINI IZ SREDNJE OGLJIČNEGA JEKLA

P. Keerthivasan[1], S. M. Sivagami[2*], T. Raja Vijay[2], N. Annamalai[3]

[1]Faculty of Mechanical Engineering, Sudharsan Engineering College, Pudukkottai, Tamilnadu, India
[2]Faculty of Mechanical Engineering, Alagappa Chettiar Government College of Engineering & Technology, Karaikudi, Tamilnadu, India
[3]Faculty of Mechanical Engineering, Government College of Engineering, Srirangam, Trichy, Tamilnadu, India

Prejem rokopisa – received: 2024-08-20; sprejem za objavo – accepted for publication: 2024-11-30

doi:10.17222/mit.2024.1281

This study presents a compelling exploration of the microstructural and mechanical enhancements achieved with Inconel 718 hardfaced layers on AISI 1045 medium carbon steel through the advanced cold metal transfer (CMT) process. By precisely adjusting process parameters such as travel speed and wire feed rate, this research examines their effects on bead geometry and dilution for both stringer- and oscillation-type depositions. Microstructural analysis unveiled defect-free hardfaced layers, achieving seamless metallurgical bonding between the substrate and hardfacing material. Notably, oscillation-type deposition with optimized parameters (6 m/min wire feed rate and 20 cm/min travel speed) achieved an impressively low dilution of 3.38 %, surpassing stringer-type deposition in quality. Furthermore, hardness testing highlighted a significant improvement in the surface durability as oscillation-type deposition reached 254 HV, while the value of the substrate was 172 HV. SEM-EDX analysis confirmed the inclusion of critical alloying elements such as nickel, niobium, and molybdenum, reinforcing the hardfaced layer's robust composition. These findings underscore the CMT process's capacity to fabricate high-quality, low-dilution Inconel 718 hardfaced layers, providing substantial resistance to corrosion and wear. The finely tuned parameters identified here offer valuable guidance for the industries seeking enhanced performance in demanding environments.

Keywords: cold metal transfer (CMT), Inconel 718, hardfacing, process parameters, bead geometry

V članku avtorji opisujejo študijo karakterizacije mikrostrukture in mehanskih lastnosti nastalih s platiranjem Ni superzlitine Inconel 718 na podlago iz srednje ogljičnega jekla AISI 1045. Postopek platiranja oziroma navarjanja so izvedli z naprednim postopkom prenosa kapljic raztaljene kovine s kovniske elektrode na hladno kovinsko podlago (CMT; angl.: Cold Metal Transfer Process). Z natančnim vodenjem procesnih parametrov, kot sta: hitrost potovanja in doziranja kovinskih kapljic z žične elektrode na kovinsko podlago, so avtorji ugotavljali vplive na geometrijo nastale posteljice in način raztapljanja tako pri oscilacijskem kot tudi nalagalnem (angl.: stringer type) načinu depozicije. Mikrostrukturna karakterizacija je pokazala, da so s poizkusi nastale trde plasti brez napak in pravo metalurško vezjo med podlago in nanešenimi trdimi tankimi plastmi. Avtorji opozarjajo, da je pri oscilacijskem tipu optimalne depozicije (doziranje žice 6 m/min in hitrost potovanja 20 cm/min) doseženo izrazito majhno raztapljanje (3,38 %) in s tem preseglo kakovost depozicije pri nalagalnem načinu depozicije. Nadalje so meritve mikrotrdote pokazale pomembno izboljšanje odpornosti proti obrabi pri trdoti trde plasti 254 HV v primerjavi s trdoto podlage, ki je bila 172 HV. SEM-EDX analize so potrdile vnos kritičnih kemijskih elementov, kot so Ni, Nb in Mo pri nastanku robustne trde plasti. Ugotovitve te študije so pokazale, da je s CMT postopkom možno izdelati visoko kakovostne trde plasti na osnovi Inconela 718 z majhnim raztapljanjem, kar pomembno izboljša odpornost izbranega jekla proti obrabi in koroziji. V zaključku avtorji povdarjajo, da njihov način uglaševanja procesnih parametrov lahko ponudi industriji nasvete, kako najti učinkovit način za doseganje ustrezne kvalitete v zahtevnih pogojih uporabe.

Ključne besede: nanašanje kapljic raztaljene kovine na hladno kovinsko podlago, Ni zlitina Inconel 718, trdo platiranje, procesni parametri, geometrija posteljice raztaljene kovine

1 INTRODUCTION

AISI 1045 carbon steel is widely used in engineering applications for transmission components that undergo fluctuating stresses. It is valued for its cost-effectiveness, ease of machining, and robust mechanical properties following quenching and tempering.[1,2] However, its relatively soft structure and limited wear resistance often lead to wear and failure under challenging conditions.[3] Rather than replacing worn components, which is costly and resource-intensive, enhancing their durability is a more sustainable solution. Researchers are focusing on extending the life of these components by applying high-quality ferrous coatings that increase the wear resistance, enabling the parts to withstand harsh environments longer. Additionally, refurbishing worn parts instead of replacing them helps reduce costs and minimize material waste.[4–6]

Cold metal transfer (CMT), a cutting-edge welding technology, is instrumental in these efforts. With precise

*Corresponding author's e-mail:
smshivagami@gmail.com (S. M. Sivagami)

Table 1: Chemical composition of the substrate and hardfacing alloy (*w*/%)

Material	Elements										
	C	Si	Mn	P	Cr	Mo	Ni	Nb	Al	Ti	Fe
Medium carbon steel	0.476	0.184	0.860	0.013	–	–	–	–	–	–	Bal
Inconel 718 filler wire	0.05	0.1	0.1	–	17.6	3.0	53.5	5.2	0.45	0.95	19.5

control over the metal transfer and minimized heat input, CMT effectively prevents heat distortion and supports a smooth operation, making it especially suited for thin and dissimilar materials like steel and aluminum.[7] Compared to traditional methods like gas metal arc welding (GMAW) or gas tungsten arc welding (GTAW), CMT offers several advantages: lower energy consumption, reduced filler material usage, and fewer post-weld treatments.[8] CMT's automation compatibility also makes it a top choice for industries like automotive, aerospace, and electronics, where repeatable high-quality welds are critical.

Developed by Fronius International, CMT is an advanced form of GMAW characterized by a lower heat input. This "cold" technique retracts the filler wire during metal transfer, significantly reducing the heat input, making it ideal for the materials with vastly different melting points, and minimizing intermetallic compounds that weaken joints.[9] This process also strengthens joints by reducing intermetallic layer thickness and producing low-dilution, durable coatings.[10,11] For example, using CMT to coat carbon-manganese steel with Inconel 625 has yielded excellent results, achieving a low, 2.45 % dilution of iron and a high deposition rate. Similarly, Inconel 718 alloy cladding, with less than 10 % dilution, is achievable with CMT, reducing the heat-affected zone (HAZ) and intermixing in nickel-based alloy coatings.[12–16]

This study examines CMT's effectiveness in applying Inconel 625 onto mild steel, analyzing how the heat flow direction affects the grain structure and how molybdenum (Mo) and niobium (Nb) enhance the microhardness and improve erosion and corrosion resistance. Mo and Nb segregate in the interdendritic regions, while hard precipitates further reinforce the cladding's resilience.[17–21] To improve the coating strength, wear resistance, and hardness, CMT's weaving techniques such as stringer beads, triangles, zigzags, spirals, and double eights spread the weld metal across a broader area, producing a wider bead with minimal heat input and dilution.[22–26]

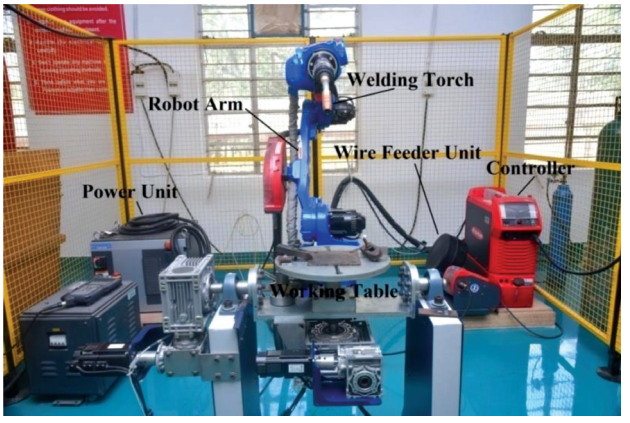

Figure 1: CMT experimental set-up

While research on the sine wave weaving in CMT is limited, this study explores its potential for Inconel 718 hardfacing on AISI 1045 medium carbon steel. By optimizing the travel speed and wire feed rate, alongside macro- and microstructural analysis and hardness testing, this investigation seeks the best bead pattern for improved performance. The findings will enhance the durability of transmission components in both onshore and offshore applications.

2 EXPERIMENTAL WORK

Medium carbon steel plates measuring (100 × 100 × 10) mm were selected as the substrate, and a 1.2 mm diameter Inconel 718 filler wire was used for hardfacing. To remove surface oxides and contaminants, the steel plates were polished with silicon carbide sandpaper and cleaned with acetone. **Table 1** provides the chemical composition of the substrate and hardfacing alloy, respectively.

The hardfacing was applied using a Fronius TPS 400i synergic CMT machine paired with a 6-axis Yaskawa Motoman robot for precise control over the travel speed and path. **Figure 1** displays the CMT experimental set-up. Argon was used as the shielding gas. Based on preliminary tests and previous research, parameters such as wire feed rate and travel speed were selected for optimal performance. Two deposition methods were applied: (a) stringer and (b) oscillation.

Hardfacing was performed by (i) varying the wire feed rate between 4 m/min and 7 m/min while keeping a travel speed of 20 cm/min, and (ii) adjusting the travel speed to 15–30 cm/min while keeping the wire feed rate at 6 m/min. The process parameters used for both deposition methods are shown in **Table 2**. The standoff distance was kept at 12 mm with an argon flow rate of 15 LPM throughout. For the bead geometry, bead width (B1), penetration depth (B2), and reinforcement height (B3) were measured, and dilution percentage (B4) was calculated using Equation (1):

$$B4 = \frac{A_p}{A_r + A_p} \times 100 \ \ (\%) \qquad (1)$$

where A_p – penetration area, A_r – reinforcement area.

Table 2: Hardfacing process parameters

Set I (Constant travel speed)				Set II (Constant wire feed rate)			
Stringer	Oscillation	Wire feed rate (m/min)	Travel speed (cm/min)	Stringer	Oscillation	Travel speed (cm/min)	Wire feed rate (m/min)
S1	O1	4	20	S5	O5	15	6
S2	O2	5		S6	O6	20	
S3	O3	6		S7	O7	25	
S4	O4	7		S8	O8	30	

Figure 2: a) CMT hardfaced layer, b) hardfaced specimen, c) geometrical view

Microstructural analysis was conducted using an RS Pro USB Digital microscope. The specimens were polished with emery paper, followed by diamond paste, and etched using Nital and Kalling's solutions. Microhardness was tested with a Mitutoyo microhardness tester at a 500-gram load and 30-second duration. Elemental composition at different zones was analyzed using a ZEISS scanning electron microscope (SEM) and Bruker energy-dispersive X-ray spectroscopy (EDX).

3 EXPERIMENTAL RESULTS AND DISCUSSION

Inconel 718 hardfaced layers were applied onto the medium carbon steel plate at two different sets of process parameters for both stringer and oscillation deposition. These process parameters were determined based on the geometrical and microstructural characteristics observed in the stringer and oscillation deposition during the experimental phase.

3.1 Macro (geometrical) investigation

Compared to the other surfacing processes, CMT applies hardfaced layers with lower heat input, minimizing distortion. However, excessive penetration depth and dilution can negatively impact the base alloy's properties and reduce the adhesion between the substrate and hardfaced materials. Thus, optimal process parameters are essential for achieving a suitable bead geometry and

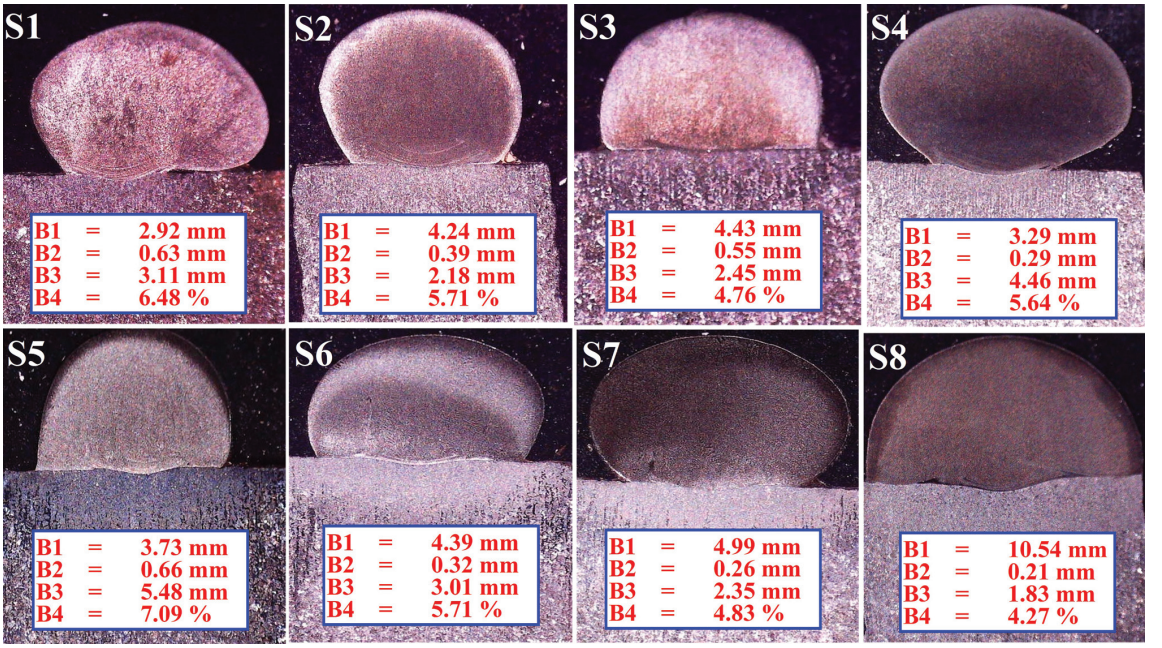

Figure 3: Macro view of bead geometry for stringer deposition

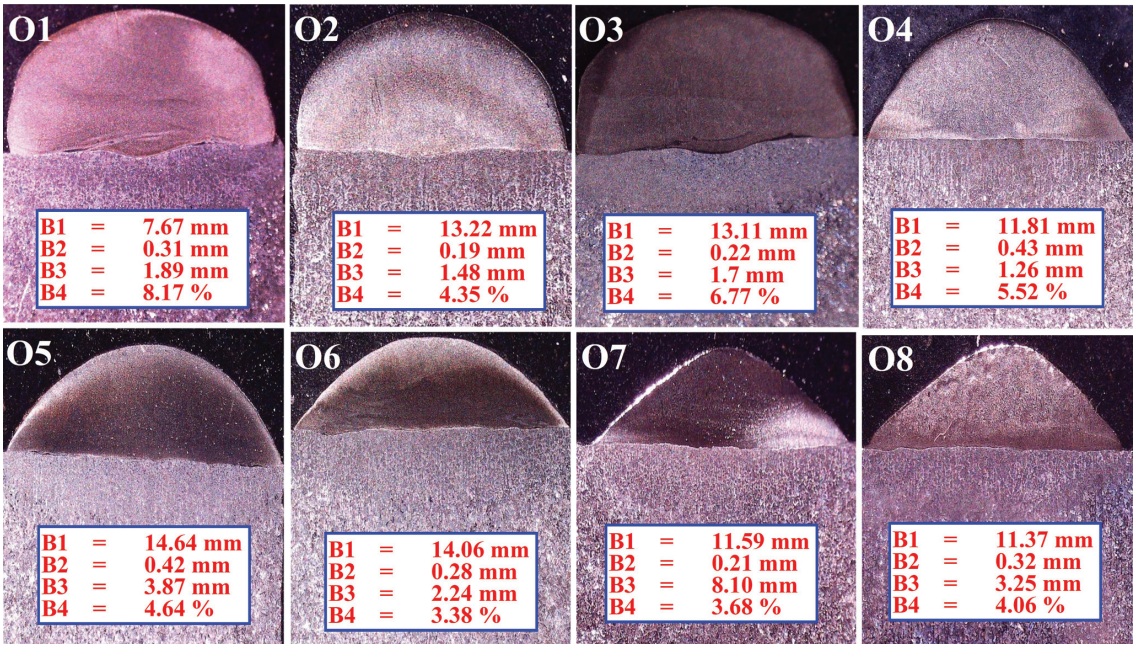

Figure 4: Macro view of bead geometry for oscillation deposition

minimize dilution. **Figure 2a** to **2c** illustrates the hardfaced layer, hardfaced specimen, and its geometry.

Figures 3 and **4** show the macro views of the bead geometry for both stringer and oscillation deposition. Defect-free hardfaced specimens were achieved with two types of bead shapes observed: (i) curved beads formed during stringer deposition and (ii) slightly flat beads formed during oscillation deposition. The amount of hardfacing material applied to the substrate depends on the application needs and can be optimized by adjusting process parameters such as wire feed rate and travel speed.

Based on the findings, the ideal criteria for hardfacing are the maximum bead width and minimal dilution, with the penetration depth and reinforcement as secondary considerations for strong bonding between the hardfaced layer and substrate.[27] **Table 3** presents the bead geometry for each specimen. For stringer deposition (Set I), an increase in the wire feed rate from 4 m/min to 6 m/min at a constant travel speed of 20 cm/min increased the bead width while reducing dilution. The optimal bead width (4.43 mm) with low dilution (4.76 %) was achieved with a wire feed rate of 6 m/min in sample S3. This result is due to the higher current increasing the heat energy, which rapidly melts the hardfacing material, forming a wide but shallow molten pool that minimizes dilution.

In oscillation deposition, a maximum bead width of 13.22 mm and low dilution of 4.35 % were obtained with a wire feed rate of 5 m/min and a travel speed of 20 cm/min in sample O2. The oscillation technique covers a larger width with minimal penetration, making it suitable for applications where reduced dilution is preferred. Overall, oscillation deposition demonstrated better control over dilution compared to stringer deposition under similar conditions.

At a constant wire feed rate of 6 m/min, increasing the travel speed from 15 cm/min to 25 cm/min led to a broader bead width and decreased dilution. Lower travel speeds produce a narrower bead with a higher liquid metal pressure on the substrate, resulting in increased dilution. Conversely, higher travel speeds reduce the amount of deposited material, forming a shallower weld bead. The maximum bead width (10.54 mm) and lowest dilution (4.27 %) were recorded in sample S8 due to a lower heat input and less material deposition, while the oscillation sample O6 achieved an even greater bead width (14.06 mm) and even lower dilution (3.38 %).

In summary, experiment O6 consistently achieved the maximum bead width and minimum dilution with both parameter sets, and samples S8 and O6 were selected for further microstructural analysis.

Table 3: Hardfaced specimens' bead geometry parameters

Set I (Constant travel speed)					Set II (Constant wire feed rate)				
Bead	B1 (mm)	B2 (mm)	B3 (mm)	B4 (%)	Bead ID	B1 (mm)	B2 (mm)	B3 (mm)	B4 (%)
S1	2.92	0.63	3.11	6.48	S5	3.73	0.66	5.48	7.09
S2	4.24	0.39	2.18	5.71	S6	4.39	0.32	3.01	5.71
S3	4.43	0.55	2.45	4.76	S7	4.99	0.26	2.35	4.83
S4	3.29	0.29	4.46	5.64	S8	10.54	0.21	1.83	4.27
O1	7.67	0.31	1.89	8.17	O5	14.64	0.42	3.87	4.64
O2	13.22	0.19	1.48	4.35	O6	14.06	0.28	2.24	3.38
O3	13.11	0.22	1.7	6.77	O7	11.59	0.21	8.10	3.68
O4	11.81	0.43	1.26	5.52	O8	11.37	0.32	3.25	4.06

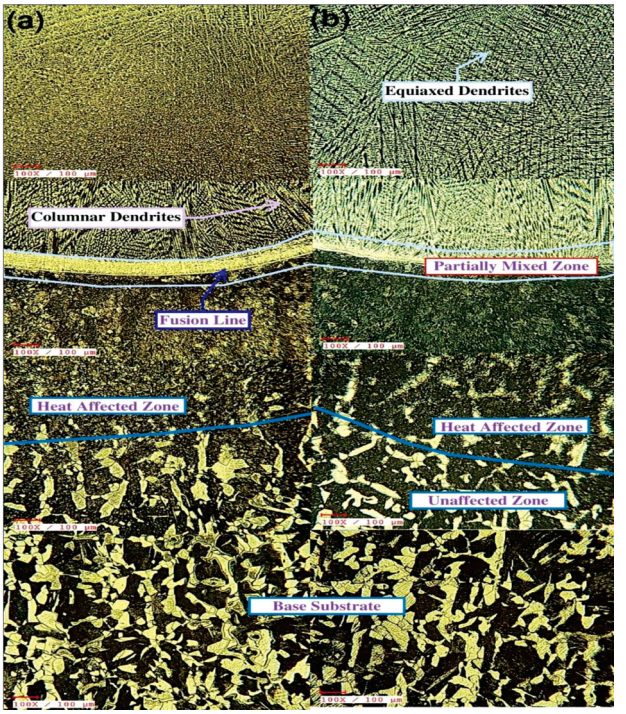

Figure 5: Microstructures of hardfaced specimens: a) stringer and b) oscillation deposition

3.2 Microstructure evolution of hardfaced Inconel 718

Microstructural analysis was conducted on different zones of the hardfaced specimens, as shown in **Figure 5**. The lower region, representing the substrate, displays ferrite and pearlite grains. In contrast, the upper region of the Inconel 718 hardfaced layer exhibits an equiaxed dendritic microstructure, enhancing the mechanical properties.

The heat from the molten wire softens the base material at the interface zone, leading to coarser grains in the HAZ. Due to the low heat input of the CMT technique, intergranular liquation and the HAZ size are reduced.[28] Between the substrate and hardfacing material lies a partially mixed zone (PMZ), where liquid Inconel 718 interfaces with solid AISI 1045. This PMZ, a critical boundary separating the substrate and weld material, is smaller with oscillation deposition compared to stringer deposition. Monitoring this zone is essential for tracking compositional changes in the substrate and hardfacing layer.

The material composition significantly influences solidification morphology, affecting the thermal conductivity of the hardfacing layer and consequently influencing constitutional supercooling. This supercooling affects the solidification morphology, particularly in stringer beads, where increased heat accumulation slows cooling, widening the spacing between dendritic arms. At the interface, columnar grains develop, but they transition to fine equiaxed grains near the upper surface of the hardfaced layer (**Figure 5a**). The oscillation deposition technique, which involves torch movement to control transverse flow and create swirling, accelerates cooling rates. This results in reduced secondary arm spacing, as shown in **Figure 5b**. Equiaxed dendrites in the hardfaced layer align orthogonally to the substrate, oriented opposite to the direction of heat flow during solidification.[29]

3.3 Microhardness evaluation of hardfaced specimens

Microhardness is a key indicator of performance of hardfaced coatings, providing essential insights into material resilience. **Figure 6** shows the microhardness profiles of both stringer and oscillation deposition methods, with measurements taken across the unaffected zone (UAZ), heat affected zone (HAZ), interface zone (IZ), and hardfaced zone (HZ). The analysis shows consistently high hardness values in the hardfaced zone for both deposition techniques.

For oscillation deposition, microhardness measurements reveal a smooth distribution of heat input, achieving a maximum hardness of 254 HV in the hardfaced zone and a minimum of 172 HV in the unaffected zone (substrate). This elevated hardness in the hardfaced layer, compared to the substrate, is attributed to specific chemical elements, such as Nb, Ni, Cr, C, and an abundance of carbides formed during the final solidification stage. These carbides play a critical role in inhibiting dislocation movement at grain boundaries, thereby enhancing material strength and hardness.

A gradual decrease in the hardness is noted from the Inconel 718 hardfaced layer towards the substrate, with the CMT process reaching peak temperatures near the fusion zone (FZ). The thermal effects of hardfacing lead to a coarser grain structure in the HAZ, resulting in a lower hardness than that of the FZ or HZ, yet higher than that of the substrate. The PMZ, blending characteristics of both the HAZ and HZ, marks a transition in hardness,

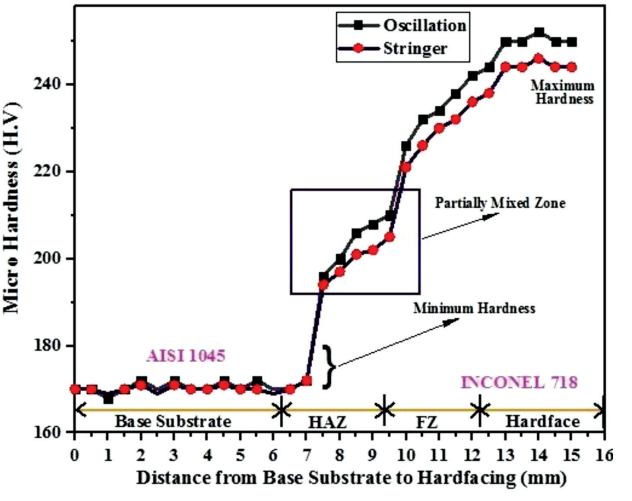

Figure 6: Microhardness profiles of hardfaced specimens for stringer and oscillation deposition

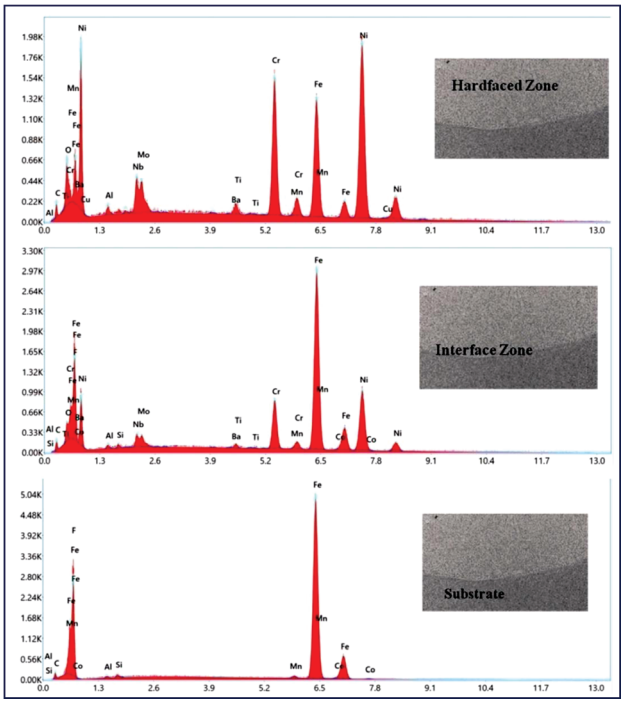

Figure 7: SEM-EDX spectra of a hardfaced specimen

reflecting the gradual shift from the substrate to hardfaced region properties.

This detailed microhardness evaluation highlights the effectiveness of oscillation deposition in achieving a robust hardfaced layer, which ultimately strengthens the coating and enhances its wear resistance.

3.4 SEM micrographs with an EDX analysis of a hardfaced specimen

Figure 7 presents the SEM-EDX analysis of a hardfaced specimen. In the initial stage, there is a significant transfer of elements between the hardfaced layer and the substrate. The overlay process increases the iron concentration in the hardfaced zone compared to the base metal. When Inconel 718 is deposited onto medium carbon steel, the niobium concentration tends to decrease in the interface zone due to (i) dilution, restricted diffusion of elements, and phase transformation, and (ii) the reaction of nickel with iron and carbon. In the hardfaced zone, the niobium concentration remains higher than in the interface zone because niobium tends to form stable niobium carbides (NbC).

The formation of primary dendrites (γ) within the hardfaced layer is driven by heat buildup, a slower solidification rate, and the depletion of niobium and carbon. Carbide growth is influenced by the volume of carbon diffusion. When niobium reaches the eutectic composition, a Laves phase begins to develop, as shown in **Figure 8**. The concentration of the Laves phase and NbC is determined by the carbon-to-niobium ratio.[30–32] A lower ratio results in reduced concentrations of the Laves phase and NbC. Other alloying elements, apart from niobium,

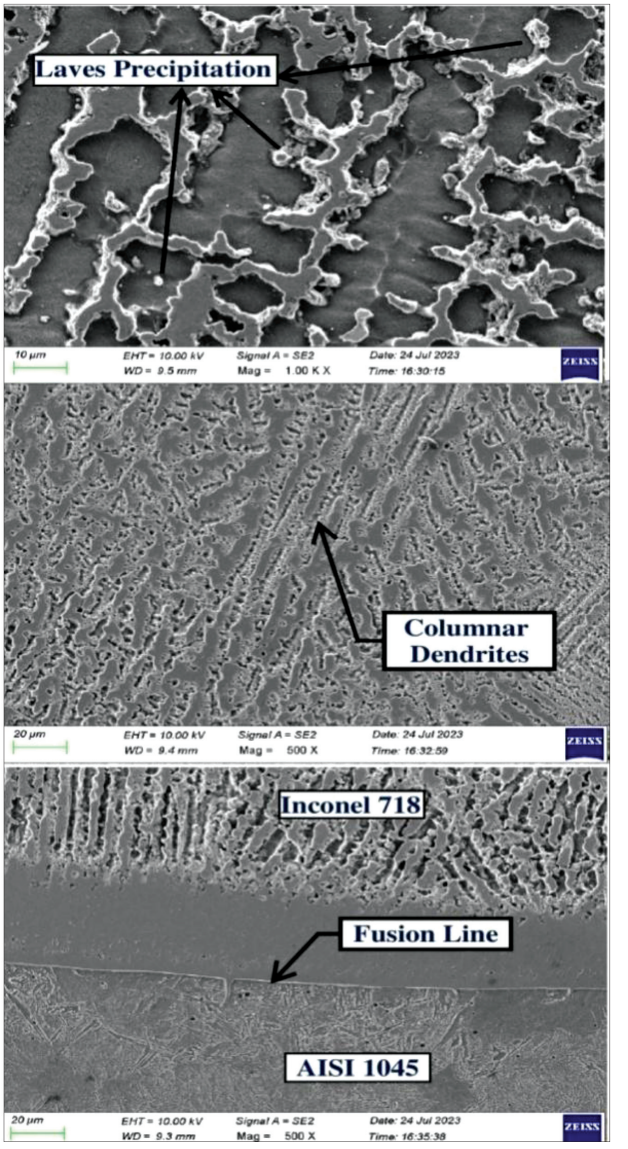

Figure 8: SEM morphology of a hardfaced specimen

also affect the formation of the Laves phase, with solubility limits and the segregation behavior of these elements playing crucial roles.[33–35]

SEM-EDX analysis in **Figure 7** shows the segregation of alloying elements such as Fe, Cr, Ni, Si, and Ti in the γ matrix. Mo and Nb, due to their high segregation tendencies, exhibit higher concentrations within the Laves phase and interdendritic zones.[36–39]

4 CONCLUSION

The CMT process has proven to be an effective method for hardfacing Inconel 718 onto medium carbon steel. This study's findings highlight the key outcomes that make this approach a valuable solution for restoring and enhancing medium carbon steel components used in transmission systems across various industries.

The hardfacing of Inconel 718 produced defect-free components, demonstrating its suitability for the repair of worn or service-damaged carbon steel-based parts in transmission applications.

The macrostructural analysis revealed distinct fusion characteristics: while stringer beads showed curved fusion, oscillation beads exhibited flat fusion. Notably, oscillation deposits achieved a maximum bead width and lower dilution percentage at optimal parameters (6 m/min wire feed rate and 20 cm/min travel speed), further enhancing the quality of the hardfacing.

The microstructural analysis confirmed a robust metallurgical bond between the Inconel 718 layer and the medium carbon steel substrate, with a defect-free, crack-resistant bead structure, underscoring the process reliability.

Microhardness measurements indicated that the hardfaced zone exhibited the highest hardness (254 HV), attributed to key alloying elements Nb, Ni, Cr, and C, as well as the formation of carbides during solidification. Hardness increased progressively from the substrate (172 HV) to the hardfaced layer, highlighting a gradient in the mechanical properties.

The SEM-EDX analysis confirmed the distribution of critical elements, with niobium concentrated in interdendritic regions, and other alloying elements (Ni, Cr, Si, Ti, and Fe) more prominent in dendritic areas, contributing to enhanced wear resistance.

Oscillation hardfacing demonstrated a superior microstructure, increased hardness, and stronger bonding, making it the preferred technique for surface restoration in demanding conditions.

In conclusion, CMT-based Inconel 718 hardfacing provides a durable, high-performance solution for extending the lifespan of medium carbon steel components, providing significant benefits for applications requiring enhanced surface resilience and wear resistance.

Nomenclature:

CMT – Cold metal transfer
GMAW – Gas metal arc welding
GTAW – Gas tungsten arc welding
HAZ – Heat affected zone
LPM – Litre per minute
B1 – Bead width
B2 – Penetration depth
B3 – Reinforcement height
B4 – Dilution percentage
SEM – Scanning electron microscope
EDX – Energy-dispersive X-ray spectroscopy
A_p – Penetration area
A_r – Reinforcement area
PMZ – Partially mixed zone
UAZ – Unaffected zone
HAZ – Heat affected zone
IZ – Interface zone
HZ – Hardfaced zone
FZ – Fusion zone
NbC – Niobium carbide

Acknowledgments

The authors acknowledge Mr. M. Sathish Kumar for his assistance with the experimental work and for providing additional support in utilising the CMT set-up provided by the Centre of Excellence on Smart Manufacturing at Alagappa Chettiar Government College of Engineering and Technology in Karaikudi, Tamilnadu, India.

5 REFERENCES

[1] Y. Lu, H. Li, H. Zhang, G. Huang, H. Xu, Z. Qin, X. Lu, Zr-based metallic glass coating for corrosion resistance improvement of 45 steel, Mater. Trans., 58 (**2017**) 9, 1319–1321, doi:10.2320/matertrans.M2017118

[2] G. Huang, L. Qu, Y. Lu, Y. Wang, H. Li, Z. Qin, X. Lu, Corrosion resistance improvement of 45 steel by Fe-based amorphous coating, Vacuum, 153 (**2018**), 39–42, doi:10.1016/j.vacuum.2018.03.042

[3] P. Xu, C. Lin, C. Zhou, X. Yi, Wear and corrosion resistance of laser cladding AISI 304 stainless steel/Al_2O_3 composite coatings, Surf. Coat. Technol., 238 (**2014**), 9–14, doi:10.1016/j.surfcoat.2013.10.028

[4] Y. Sui, F. Yang, G. Qin, Z. Ao, Y. Liu, Y. Wang, Microstructure and wear resistance of laser-cladded Ni-based composite coatings on downhole tools, J. Mater. Process. Technol., 252 (**2018**), 217–224, doi:10.1016/j.jmatprotec.2017.09.028

[5] L. Zhu, S. Wang, H. Pan, C. Yuan, X. Chen, Research on remanufacturing strategy for 45 steel gear using H13 steel powder based on laser cladding technology, J. Manuf. Processes, 49 (**2020**), 344–354, doi:10.1016/j.jmapro.2019.12.009

[6] X. Chen, M. Yao, F. Kong, Y. Fu, J. Wu, H. Zhang, In-situ quality monitoring of laser hot wire cladding process based on multi-sensing diagnosis and machine learning model, J. Manuf. Process., 87 (**2023**), 183–198, doi:10.1016/j.jmapro.2023.01.031

[7] A. A. Siddiqui, A. Kumar Dubey, Recent trends in laser cladding and surface alloying, Opt. Laser Technol., 134 (**2021**), 106619, doi:10.1016/j.optlastec.2020.106619

[8] G. P. Rajeev, M. Kamaraj, S. R. Bakshi, Hard-facing of AISI H13 tool steel with Stellite 21 alloy using cold metal transfer welding process, Surf. Coat. Technol., 326 (**2017**), 63–71, doi:10.1016/j.surfcoat.2017.07.050

[9] C. G. Pickin, K. Young, Evaluation of cold metal transfer (CMT) process for welding aluminium alloy, Sci. Technol. Weld. Joi., 11 (**2006**) 5, 583–585, doi:10.1179/174329306X120886

[10] H. T. Zhang, J. C. Feng, P. He, B. B. Zhang, J. M. Chen, L. Wang, The arc characteristics and metal transfer behaviour of cold metal transfer and its use in joining aluminium to zinc-coated steel, Mater. Sci. Eng.: A, 499 (**2009**) 1–2, 111–113, doi:10.1016/j.msea.2007.11.124

[11] G. Lorenzin, G. Rutili, The innovative use of low heat input in welding: experiences on cladding and brazing using the CMT process, Weld. Int., 23 (**2009**) 8, 622–632, doi:10.1080/09507110802543252

[12] G. P. Rajeev, M. Kamaraj, S. R. Bakshi, Al-Si-Mn Alloy Coating on Aluminum Substrate Using Cold Metal Transfer (CMT) Welding Technique, JOM, 66 (**2014**), 1061–1067, doi:10.1007/s11837-014-0970-7

[13] C. G. Pickin, S. W. Williams, M. Lunt, Characterisation of the cold metal transfer (CMT) process and its application for low dilution cladding, J. Mater. Proc. Technol., 211 (**2011**) 3, 496–502, doi:10.1016/j.jmatprotec.2010.11.005

[14] O. T. Ola, F. E. Doern, A study of cold metal transfer clads in nickel-base Inconel 718 superalloy, Mater. Des., 57 (**2014**), 51–59, doi:10.1016/j.matdes.2013.12.060

[15] P. Varghese, E. Vetrivendan, M. Kumar Dash, S. Ningshen, M. Kamaraj, U. Kamachi Mudali, Weld overlay coating of Inconel 617 M on type 316 L stainless steel by cold metal transfer process, Surf. Coat. Technol., 357 (**2019**), 1004–1013, doi:10.1016/j.surfcoat.2018.10.073

[16] D. T. Sarathchandra, M. J. Davidson, Effect of heat input on mechanical and microstructural properties of Inconel 625 depositions processed in wire arc additive manufacturing, Proc. Inst. Mech. Eng. Part E: J. Process. Mech. Eng., 235 (**2021**) 5, 1439–1448, doi:10.1177/09544089211004718

[17] M. Solecka, A. Kopia, A. Radziszewska, B. Rutkowski, Microstructure, microsegregation and nanohardness of CMT clad layers of Ni-base alloy on 16Mo3 steel, J. Alloys Compd., 751 (**2018**), 86–95, doi:10.1016/j.jallcom.2018.04.102

[18] T. Zhao, S. Zhang, Z. Y. Wang, C. H. Zhang, D. X. Zhang, N. W. Wang, C. L. Wu, Cavitation erosion/corrosion synergy and wear behaviors of nickel-based alloy coatings on 304 stainless steel prepared by cold metal transfer, Wear, 510 (**2022**), 204510, doi:10.1016/j.wear.2022.204510

[19] J. Ghosh Roy, N. Yuvaraj & Vipin, Effect of welding parameters on mechanical properties of cold metal transfer welded thin AISI 304 stainless-steel sheets, Trans. Indian Inst. Metals, 74 (**2021**), 2397–2408, doi:10.1007/s12666-021-02326-2

[20] X. Tang, S. Zhang, X. Cui, C. Zhang, Y. Liu, J. Zhang, Tribological and cavitation erosion behaviors of nickel-based and iron-based coatings deposited on AISI 304 stainless steel by cold metal transfer, J. Mater. Res. Technol., 9 (**2020**) 3, 6665–6681, doi:10.1016/j.jmrt.2020.04.064

[21] S. Singh Sandhu, A. S. Shahi, Metallurgical, wear and fatigue performance of Inconel 625 weld claddings, J. Mater. Process. Technol., 233 (**2016**), 1–8, doi:10.1016/j.jmatprotec.2016.02.010

[22] J. Tapiola, J. Tuominen, J. Vihinen, P. Vuoristo, Sliding wear behavior of cold metal transfer cladded Stellite 12 hard-facings on martensitic stainless steel, Weld. World, 67 (**2023**), 573–584, doi:10.1007/s40194-022-01390-6

[23] C. Carvalho Silva, E. Cordeiro de Miranda, M. Ferreira Motta, H. Cordeiro de Miranda, J. Pereira Farias, Minimization of defects in nickel based superalloy weld overlay deposited by the GTAW cold wire feed process, Weld. Int., 30 (**2016**) 6, 443–451, doi:10.1080/09507116.2015.1096558

[24] N. Pravin Kumar, N. Siva Shanmugam, Some studies on nickel based Inconel 625 hard overlays on AISI 316L plate by gas metal arc welding based hard-facing process, Wear, 456 (**2020**), 203394, doi:10.1016/j.wear.2020.203394

[25] S. Gejendhiran, A. Karpagaraj, D. Vinoth Kumar, Ragupathy Dhanusuraman, N. Annamalai, Experimental investigations on Inconel 718 hard-faced layer deposited over SS304 using cold metal transfer, Surf. Coat. Technol., 468 (**2023**), doi:10.1016/j.surfcoat.2023.129739

[26] L. Sexton, S. Lavin, G. Byrne, A. Kennedy, Laser cladding of aerospace materials, J. Mater. Proc. Technol., 112 (**2002**) 1, 63–68, doi:10.1016/S0924-0136(01)01121-9

[27] G. Liu, S. Zhou, P. Lin, X. Zong, Z. Chen, Z. Zhang, L. Ren, Analysis of microstructure, mechanical properties, and wear performance of NiTi alloy fabricated by cold metal transfer based wire arc additive manufacturing, J. Mater. Research and Technol., 20 (**2022**), 246–259, doi:10.1016/j.jmrt.2022.07.068

[28] A. Evangeline, P. Sathiya, Dissimilar cladding of Ni–Cr–Mo superalloy over 316 austenitic stainless steel: morphologies and mechanical properties, Met. Mater. Int., 27 (**2021**), 1155–1172, doi:10.1007/s12540-019-00440-x

[29] P. N. Quested, M. McLean, Effect of variations in temperature gradient and solidification rate on microstructure and creep behaviour of IN 738LC, Proc. Conf. on 'Solidif. technol. foundry cast house', (**1983**), 586–591

[30] H. Kim, W. Cong, H. C Zhang, Z. Liu, Laser engineered net shaping of nickel-based superalloy Inconel 718 powders on to AISI 4140 alloy steel substrates: Interface bond and fracture failure mechanism, Materials, 10 (**2017**) 4, 341, doi:10.3390/ma10040341

[31] A. Hirose, K. Sakata, K. F. Kobayashi, Microstructure and mechanical properties of laser beam welded Inconel 718, Int. J. Mater. Prod. Technol., 13 (**2014**) 1–2, 28–44, doi:10.1504/IJMPT.1998.036226

[32] M. J. Cieslak, T. J. Headley, G. A. Knorovsky, A. D. Roming, T. Kollie, A comparison of the solidification behavior of INCOLOY 909 and INCONEL 718, Metall. Trans. A, 21 (**1990**), 479–488, doi:10.1007/BF02782428

[33] Ch. Radhakrishna, K. Prasand Rao, S. Srinivas, Laves phase in superalloy 718 weld metals, J. Mater. Sci. Lett., 14 (**1995**), 1810–1812, doi:10.1007/BF00271015

[34] J. Schirra, R. H. Caless, R. Hatala, The Effect of Laves Phase on the Mechanical Properties of Wrought and Cast + HIP Inconel 718, Superalloys, (**1991**), 375–388, doi:10.7449/1991/SUPERALLOYS_1991_375_388

[35] K. Singh, H, Shankar, A. P Singh, Mechanical and Microstructural Properties of CMT Welded Ferritic AISI 1080 Carbon Steel (UNS G10800), In: S. Yadav, Y. Shrivastava, S. Rab (eds), Recent Advances in Mechanical Engineering, ICMET 2023, Lecture Notes in Mechanical Engineering, Springer, Singapore, (**2024**), 221–233, doi:10.1007/978-981-97-4947-8_19

[36] V. Mishra, N. Yuvaraj & Vipin, A study on the performance of super duplex stainless steel cladding over mild steel using a CMT welding, J. Adhes. Sci. Technol., (**2024**), 1–18, doi:10.1080/01694243.2024.2396120

[37] I. Bunaziv, X. Ren, A. B. Hagen, E. W. Hovig, I. Jevremovic, S. G. Dahl, Laser beam remelting of stainless steel plate for cladding and comparison with conventional CMT process, Int. J. Adv. Manuf. Technol., 127 (**2023**), 911–934, doi:10.1007/s00170-023-11567-y

[38] S. T. Selvamani, M. Bakkiyaraj, G. Yoganandan, N. Dilip Raja, An empirical study of CMT-welded interface features and corrosion characteristics of dissimilar joints, Proc. Inst. Mech. Eng., Part E: J. Process Mech. Eng., (**2023**), doi:10.1177/09544089231170986

[39] M. Emami, S. H. Elahi, M. Mashhadgarme, Effect of cold metal transfer (CMT) on the unmixed zone formation in Stellite 6 overlays on ferritic steels, Can. Metall. Q., 63 (**2023**) 4, 1704–1711, doi:10.1080/00084433.2023.2281200